GQ07: Securing Groundwater Quality in Urban and Industrial Environments (Proc. 6th International Groundwater Quality Conference held in Fremantle, Western Australia, 2–7 December 2007). IAHS Publ. 324, 2008.

Density-driven seawater plumes in a shallow aquifer caused by a flooding event – field observations, consequences for geochemical reactions and potentials for remediation schemes

M. S. ANDERSEN[1], R. JAKOBSEN[2], V. NYVANG[3], F. D. CHRISTENSEN[4], P. ENGESGAARD[5] & D. POSTMA[2]

1 *Water Research Laboratory, School of Civil and Environmental Engineering, University of New South Wales,110 King St, Manly Vale, 2093, New South Wales, Australia*
m.andersen@wrl.unsw.edu.au

2 *Environment & Resources DTU, Technical University of Denmark*

3 *Watertech/Birch og Krogboe, Teknikerbyen 34, DK-2830 Virum, Denmark*

4 *Ramboll Denmark, Bredevej 2, DK-2850 Virum, Denmark*

5 *Department of Geography and Geology, University of Copenhagen, Øster Voldgade 10, DK-1350 K, Denmark*

Abstract This study presents field and modelling data of how dense seawater plumes move into a shallow coastal freshwater aquifer, following a storm flooding event. The locations of these seawater plumes appear to be controlled by topographical depressions where seawater ponds were observed after the flooding. The rapid development and sinking of these seawater plumes in the aquifer were monitored by pore water electrical conductivity measurements in a 120-m transect of about 100 piezometers, and by drive-point continuous vertical resistivity logs (el-logs). Large parts of the plumes reached the bottom of the aquifer 10 mbs in less than 30 days, but the plume migration caused by the unstable density distribution was found to be highly variable. The variable density code SUTRA was used for numerical modelling of the flow of seawater down into the aquifer. The model captures the overall trends of the plume development and migration velocity observed in the field. However, even after introducing measured medium-scale heterogeneity in the model, it could not adequately describe the complex details in the seawater distribution. This variability is believed to be caused by the geological heterogeneity and much of the variability appears to be on a small scale (~ cm), finer than the sampling scale of this study. The vastly different chemical composition of the seawater compared to the fresh groundwater triggered several geochemical reactions in the affected part of the aquifer. The high seawater sulfate content shifted the dominating redox-process from methanogenesis to sulfate reduction. The results of this field and modelling study highlight the complexity of how an aquifer, subject to seawater flooding, is contaminated by seawater. In turn, the results give insight into the vulnerability of coastal freshwater aquifers to catastrophic flooding events and to future sea-level rise. The study also indicates how other groundwater contaminants in dense fluids released at the surface may spread in the aquifer, and, points to the possible use of density-driven flow as a novel method to introduce reactants for remediation at contaminated sites.

Key words coastal zone; density-driven flow; modelling; geochemistry; remediation

INTRODUCTION

Polluted groundwater will ultimately discharge at surface water recipients (i.e. streams, lakes and coastal waters), if the pollutant is not terminally attenuated or intercepted by abstraction wells. At the discharge zone, the outflow of contaminated groundwater is often complex due to heterogeneous geology and temporally-varying water levels in the receiving water body. In the coastal zone, the discharge is further complicated by the dynamics of the seawater–freshwater interface. Furthermore, mixing with the subsurface seawater can have consequences for geochemical processes and the fate of contaminants.

The flow and transport processes occurring when dense seawater is overlying freshwater have been studied extensively in the past by numerical modelling and laboratory experiments. However, there appears to be a lack of field data describing this complex flow and transport in real systems. Therefore, little is known about the vulnerability of coastal freshwater aquifers subject to seawater flooding with regard to the rate of seawater contamination and chemical effects on groundwater quality.

Traditionally, the coastal seawater–freshwater interface has been depicted as a landward dipping wedge of denser saline water (Kohout, 1964; Bear *et al*., 1999) maintained by a slow landward advection of seawater (Sanford & Konikow, 1989). The interface has been described as a relatively narrow mixing zone where reactions between the seawater and discharging freshwater could take place. In recent years, this conceptual understanding has been changed for coastal aquifers with sloping beaches and temporal fluctuating seawater levels (i.e. tides, wave run-up and set-up). Several field investigations have shown that the interface is much more dynamic, with fast circulation of seawater in the upper part of the beach (Turner & Acworth, 2004; Robinson *et al.*, 2006). Modelling studies have revealed that this circulation is largely driven by the tidal variation (Robinson *et al*., 2007). The modelling of the interface as a function of a predictably oscillating seawater boundary condition in turn suggests a relatively predictable configuration of the interface. However, stochastic random perturbations of the sea-level, as caused by storms, may (albeit less frequent) have a greater impact on the configuration of the seawater–freshwater interface. This may cause transient variations in the distribution of seawater and impair the prediction of the interface. In turn, such variations potentially also affect geochemical reactions and the fate of discharging contaminants.

In this paper we present field data showing the effects of a storm and flooding event on the configuration of the seawater–freshwater interface in a coastal aquifer. In addition, we show how the resulting downwards flow of dense seawater plumes changes the chemical conditions in the affected part of the aquifer.

METHODOLOGY

The field site (Fig. 1) is a coastal meadow on Zealand (Denmark) facing a brackish fjord, with a salinity of around 17‰ (details in Andersen *et al.*, 2005). During the 29th and 30th of January 2000 a storm flooded part of the coastal meadow with seawater.

About 100 piezometers were installed along a 120 m transect line aligned with the natural groundwater flow (Fig. 1(a)). The piezometers were installed with a Geoprobe 54 DT drilling rig with screens at depths ranging between 2–10 mbs (see dots in

Fig. 2(a) for locations). They were constructed from OD 25 mm polyethylene pipes and each equipped with a 12 cm screen. Hydraulic head and pore water electrical conductivity (EC) were measured frequently and the piezometers were slug tested in order to determine the permeability. Depth profiles of formation electrical conductivity (el-logs) were obtained with a Geoprobe (54 DT) driving a SC400 log-tool: an array of four electrodes, 25.4 mm apart mounted just behind the drive point. Measurements were conducted every 15 mm. The location of the el-logs is shown in Fig. 1. Three el-logs (1, 2 and 5 in Fig. 1(a)) were drilled on the 12 July 1999 before the flooding event and three (2, 3 and 4 in Fig. 1(a)) were drilled on the 2 March 2000, 32 days after the storm. Thus the el-log at location 2 was done twice.

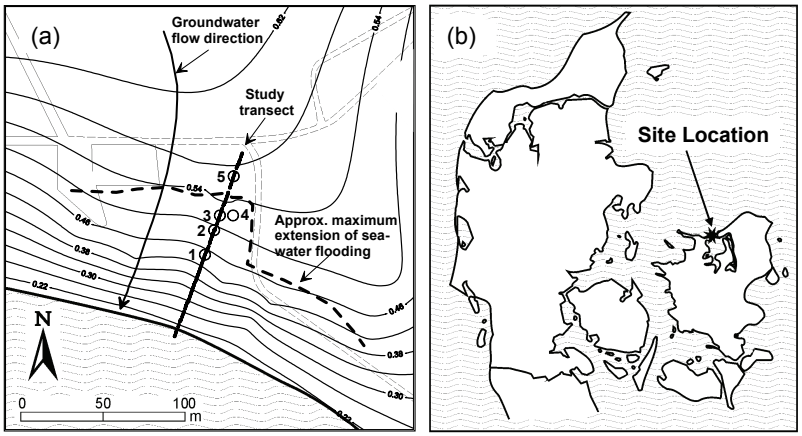

Fig. 1 (a) Location of the study transect; contour lines indicate the piezometric head (m). (○) denote locations of el-log profiles. (b) Site location at the Skansehage peninsula, Denmark.

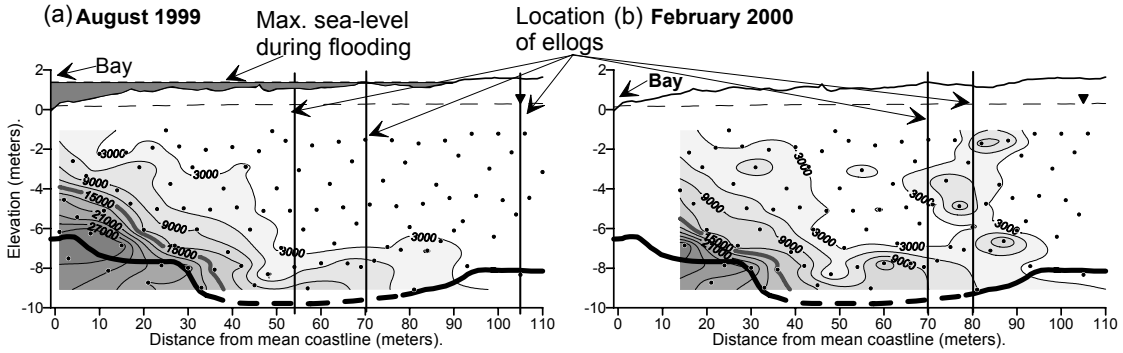

Fig. 2 Vertical cross-section of pore water electrical conductivity (μS/cm) along the study transect: (a) on 28 August 1999, and (b) on 27 February 2000. The 15 000 μS/cm contour represents 50% seawater. The thick black line indicates the location of the bottom peat layer, dashed where uncertain or missing. The vertical lines show locations where el-log profiles were drilled.

Groundwater quality samples were collected from the transect piezometers before (August 1999) and after the storm (March 2000). The samples were collected by a gas-displacement technique using nitrogen gas (Andersen *et al.*, 2005) and filtered through a 0.2 μm filter. Field analysis was done for EC, O_2, pH, alkalinity (Gran-titration) and ferrous iron (Fe^{2+}) (Ferrozine method). Samples for major cation analysis were preserved with 2% 7 M nitric acid and later analysed by Atomic Absorption

Spectroscopy (AAS). Samples for chloride and sulfate were frozen and later analysed by Ion Chromatography (IC). Sulfide samples were filtered directly into 5 ml vials containing 2 ml of a 4% Zn-acetate solution, refrigerated and later analysed spectrophotometrically by the methylene-blue method. Samples for methane (CH_4) were injected with a syringe and needle directly through a butyl rubber stopper into a weighed and pre-evacuated 10 ml Venoject glass. The vial was frozen upside down immediately after sampling, thereby trapping the gas phase. The methane content was measured in the laboratory by gas chromatography (GC).

RESULTS AND DISCUSSION

The shallow aquifer consists of about 10 m of aeolian and marine sands and gravel deposited onto a discontinuous layer of marine peat (bottom line in Fig. 2(a)). In the sand the permeability ranges from 0.25–26.5 × 10^{-11} m^2, with an average of 4.84 × 10^{-11} m^2 and a variance of 1.7 × 10^{-21} (n = 94). Thus the sands appear quite homogeneous. The topographical relief is low, varying from 0 m at the coastline to about 1.5 m at 120 m inland. The hydraulic gradient is generally seawards, varying between 0.55 and 2.75‰. Figure 2(a) shows the distribution of pore water EC, as a measure of the salinity, before the storm. The distribution of saltwater in August 1999 was found to be in reasonable agreement with the hydrological conditions at the site (Andersen, 2001; Christensen, 2002).

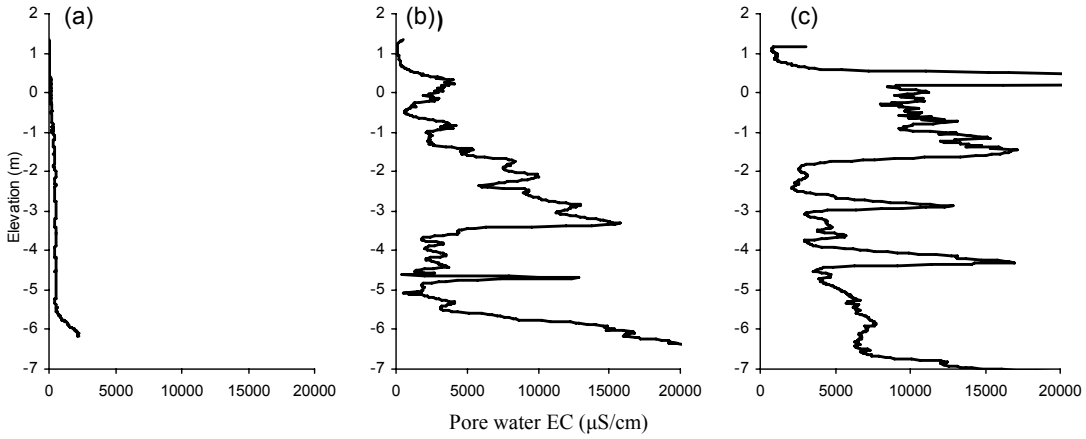

Fig. 3 Depth profiles of pore water EC derived from el-log bulk conductivity (σ_{bulk}) by applying Archies law: EC = σ_{bulk}/4.55: (a) drilled on the 12 June 1999 at site 2 (Fig. 1(a)) at 70 m from the coastline (see Fig. 2), (b) drilled on the 2 March 2000 also at site 2, (c) drilled on the 2 March 2000 at site 3 (Fig. 1(a)), 80 m from the coastline (see Fig. 2(b)).

Flooding and the sinking of dense pulses of seawater into the aquifer

During the January 2000 storm, the coastal meadow was flooded up to 90 m from the coast (Fig. 2(a)). Ponding of seawater subsequently persisted in the low lying areas in the days following the storm, causing localised percolation of dense seawater into the aquifer at these sites. Figure 2(b) shows one such seawater pulse travelling down through the aquifer 28 days after the storm. It is estimated that the first pulses might have reached the bottom in as little as 15 days. Detailed el-log profiles were drilled before and after the storm (locations in Figs 1 and 2), supplementing the pore water

measurement in the transect. Figure 3(a) and (b) show an el-log drilled twice at the same site (el-log 2), before and 32 days after the storm in the transect at 70 m from the coastline. Due to the measuring interval of 15 mm, the el-log reveals a much more detailed picture than the contoured EC distribution based on the pore water samples in Fig. 2. Before the storm (Fig. 3(a)) there is very little variation down to below 5 m. The low variability indicates homogenous aquifer material, with an average EC of 500 μS/cm representing freshwater. Below this, the conductivity increases up to 2000 μS/cm due to the toe of the seawater–freshwater interface. After the storm, several sharp peaks can be observed with conductivities up to 20 000 μS/cm (Fig. 3(b)). This complex pattern is probably the result of a complex interplay between the moderate aquifer heterogeneity and the flow induced by the unstable density distribution. Note also, the huge difference between two el-log drilled on the same day, just 10 m apart (Fig. 3(b) and (c)).

Modelling the sinking of a seawater pulse

Modelling of the downward migration of a seawater pulse was done to understand what is controlling the complex patterns seen in Figs 2 and 3. That is, are the individual peaks seen in el-logs 2 and 3 (Figs 3(b) and (c)) caused by heterogeneity (e.g. low permeable layers) or by the nature of the unstable density flow itself? The flow and transport of the pulse seen at 80 m (Fig. 3(c)) was modelled with SUTRA (Voss & Provost, 2003), using both a homogeneous and a heterogeneous permeability distribution based on a spatial analysis of slug test results (Andersen *et al*., in preparation). The model domain covers 40 m of the piezometer transect around the pulse with a depth of 10 m (see Fig. 4(a) top). The grid discretization was $\Delta x = \Delta z = 0.1$ m. The regional groundwater flow was simulated by applying a constant flux of 6.9×10^{-3} kg H_2O/s to the upstream boundary in accordance with the hydrology of the site (Andersen, 2001). For both cases, the longitudinal dispersivity (α_L) was set to 0.05 m and the transverse dispersivity (α_T) to 1/10 of the longitudinal dispersivity. An initial period of 24 h, split into timesteps of 0.5 h, represents the flooding event with a constant source of seawater at the surface (Fig. 4(a)). In the following second period, the surface source was switched off and the sinking pulse was simulated for 50 days (Δt = 1 h). The base case scenario used a homogeneous permeability of $k = 4.84 \times 10^{-11}$ m^2, the average measured value.

The homogeneous scenario did produce an unstable pulse of sinking seawater; however, it did not satisfactorily reproduce the observed field data. Instead, a mildly heterogeneous permeability distribution based on the observations was introduced (see background contours in Fig. 4(a) bottom plots). The simulation still produced unstable density flow with three distinct lobes, but compared to the homogeneous case the lobes were now partly modified by the heterogeneous permeability distribution (Fig. 4(a) bottom). The lobes moved seaward due to the ambient flow of fresh groundwater. After about 30 days the pulse reached the bottom of the aquifer and started pooling on top of the low-permeable peat (Fig. 4(a) bottom).

Figure 4(b) shows the observed salinity distribution 32 days after the storm (at 80 m) compared to the model results at 31 and 36 days at the same site. The modelled salinity profiles reproduce the observed salinity distribution in an overall sense. However, the measured salinity profile contains more variability on a small scale,

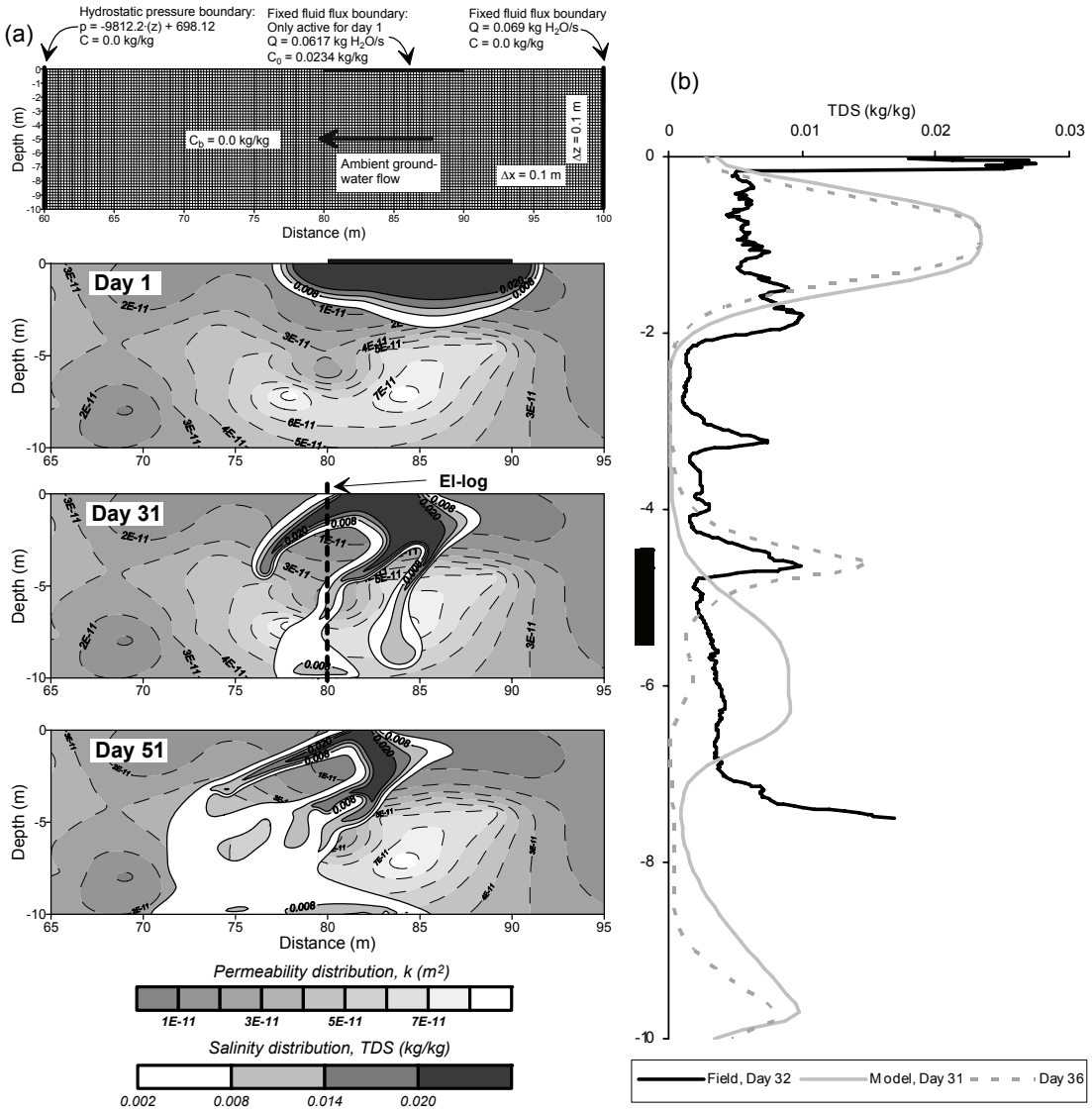

Fig. 4 (a) Modelled seawater pulse sinking through a heterogeneous permeability field. Top: model set-up. Bottom: simulated salinity distributions for days 1, 31 and 51. The permeability distribution is contoured in the background. (b) Modelled salinity depth profiles at 80 m from the coast after 31 and 36 days compared with the field salinity profile derived from the measured el-log (el-log 3, Fig. 3(c)) at 32 days after the storm.

indicating that part of the real heterogeneity has not been captured and included in the model. The modelled salinity profiles show strikingly different profiles just 5 days apart (Fig. 4(b)), highlighting that vastly different field data can be obtained by moving the sampled location by just a few metres or a few days. This underpins the difficulty or challenge in monitoring such dynamic systems in an always heterogeneous field situation. Furthermore, the huge variability illustrates that we cannot expect to be able to adequately model the effects of seawater flooding on larger stretches of coastline.

The effect of the seawater pulses on the redox-chemistry

Before the storm, groundwater in the studied transect was without oxygen or nitrate. Sulfate (Fig. 5(a)) was only detected very close to the coastline (25 m), greatly depleted

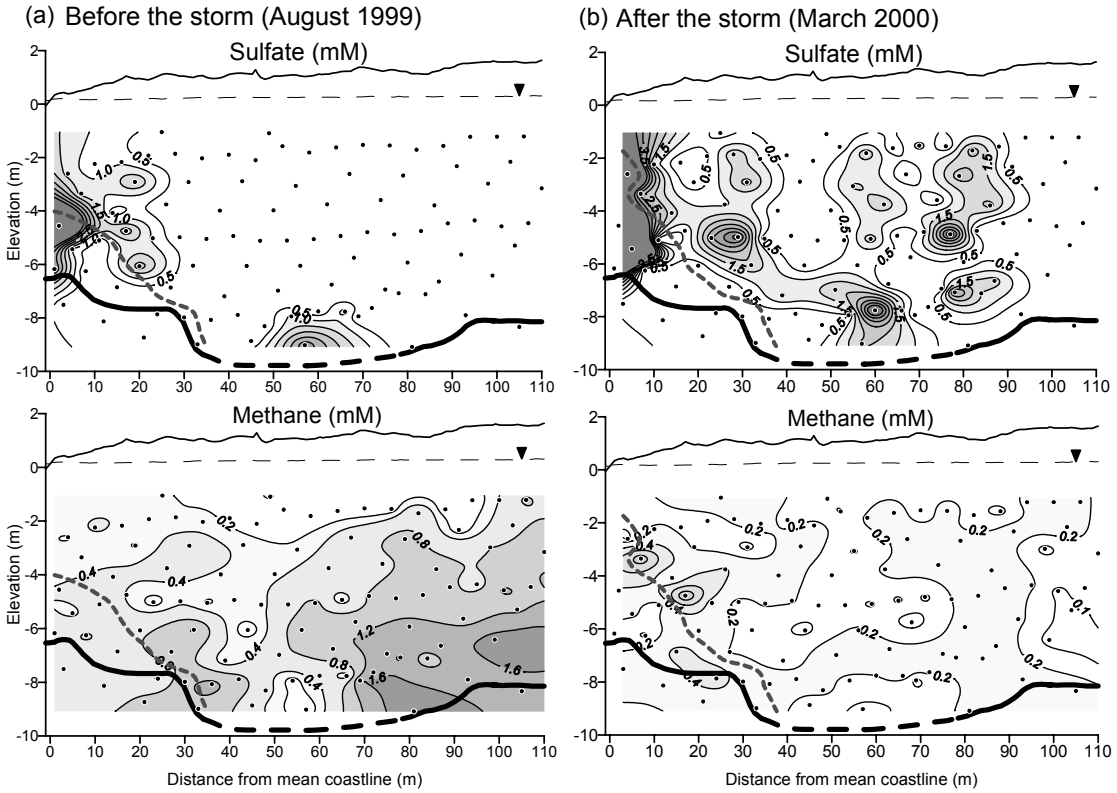

Fig. 5 Vertical chemical cross-sections showing the sulfate (mM) and methane (mM) concentrations: (a) before the storm (August 1999) and (b) after the storm (March 2000). The grey dashed line represents the 50% seawater contour (15 000 µS/cm). The thick black line indicates the location of the bottom peat layer, dashed where uncertain or missing.

relative to chloride and with sulphide concentrations up to 7.6 mM, clearly indicating substantial sulfate reduction (Andersen *et al.*, 2005). Sulfate was also present in a zone near the bottom of the aquifer at 55–65 m (Fig. 5(a)). Strontium isotope data ($^{87}Sr/^{86}Sr$) suggests that this sulfate is derived from upward leakage from the aquifer below (Jørgensen *et al*., 2007). In the landward part of the aquifer 0.5–2.0 mM of methane (Fig. 4(a)) was present and before the storm, methanogenesis was the dominating redox process in this fresher part of the transect (Nyvang, 2003). After the storm (approx. 32 days), the picture had greatly changed (Fig. 5(b)). Three distinct sulfate plumes with concentrations up to about 5 mM are seen. Two of these have reached the bottom of the aquifer. Rate measurements (Nyvang, 2003) confirmed that sulfate reduction had become the dominating redox-process after the storm. Additionally the methane concentrations are greatly diminished, possibly by oxidation by the sulfate.

The use of density-driven flow in remediation schemes?

The geochemical, physical and modelling results of the sinking seawater pulses indicate how dense fluids might be used for introducing reactive agents to contaminated sites. At contaminated coastal sites especially, adding oxidising agents to seawater, which then percolates into the aquifer, may be an acceptable solution, since the final recipient is already saline. However, the modelling indicated that it will only work effectively at sites of medium to high permeability, since lower permeability had

a tendency to stabilise the flow. Still, the denser seawater will tend to pool on top of less permeable layers, and given sufficient time, this would allow diffusion of reactants into the layers where pollutants may reside.

CONCLUSIONS

The seawater plumes created by flooding moved rapidly downwards and part of the plumes reached the bottom of the aquifer 10 mbs in less than 30 days, but, the sinking caused by the unstable density distribution was highly variable. This variability is caused by a combination of cm-scale geological heterogeneity, finer than the sampling scale of this study. After introducing medium-scale heterogeneity, the numerical model manages to capture the overall trends of the observed plume development and migration velocity. However, it could not adequately describe the complex details in the seawater distribution and spreading patterns likely produced by small-scale heterogeneities. The high seawater sulfate content shifted the dominating redox-process from methanogenic to sulfate reduction. The results of this field and modelling study highlight the complexity of how an aquifer, subject to a seawater flooding event, is contaminated by seawater. However, the study also indicates how other groundwater contaminants of high density released at the surface may spread in the aquifer, and points to the possible use of density-driven flow as a method to introduce reactants for the remediation of contaminated sites.

REFERENCES

Andersen, M. S. (2001) Geochemical processes at a seawater–freshwater interface. PhD Thesis, Technical University of Denmark, Kgs Lyngby, Denmark.

Andersen, M. S., Nyvang, V., Jakobsen, R. & Postma, D. (2005) Geochemical processes and solute transport at the seawater/freshwater interface of a sandy aquifer. *Geochim. Cosmochim. Acta* **69**(14), 3979–3994.

Andersen, M. S., Christensen, F. D., Engesgaard, P. & Jakobsen, R. (2008) Field observations and numerical modeling of density driven seawater pulses in a shallow aquifer following a flooding event at Skansehage, Denmark (in preparation).

Bear, J., Cheng, A. H. D., Sorek, S., Ouazar, D. & Herrera, I. (1999) *Seawater Intrusion in Coastal Aquifers: Concepts, Methods and Practices, Theory and Application of Transport in Porous Media*, vol. 14. Kluwer Academic Publishers, Norwell, Massachusetts, USA.

Christensen, F. D. (2002) Numerical analysis of physical and geochemical processes for seawater intrusion in coastal aquifers. PhD Thesis, Technical University of Denmark, Kgs Lyngby, Denmark.

Jørgensen, N. O., Andersen, M. S. & Engesgaard, P. (2008) Investigation of a dynamic seawater intrusion event using strontium isotopes (87Sr/86Sr). *J. Hydrol*. **348**, 257–269, doi: 10.1016/j.jhydrol.2007.10.001.

Kohout, F. A. (1964) The flow of fresh water and salt water in the Biscayne aquifer of the Miami area, Florida. *US Geol. Survey Water-Supply Paper 1613-C*, 12–32.

Nyvang, V. (2003) Redox processes at the seawater/freshwater interface in an anaerobic aquifer. PhD Thesis, Technical University of Denmark, Kgs Lyngby, Denmark.

Robinson, C., Gibbes, B. & Li, L. (2006) Driving mechanisms for groundwater flow and salt transport in a subterranean estuary. *Geophys. Res. Lett.* **33**, L03402, doi:10.1029/2005GL025247.

Robinson, C., Gibbes, B. & Li, L. (2007) Effect of tidal forcing on a subterranean estuary. *Adv. Water Resour.* **30**, 851–865, doi: 10.1016/j.advwatres.2006.07.006.

Sanford, W. E. & Konikow, L. F. (1989) Simulation of calcite dissolution and porosity changes in saltwater mixing zones in coastal aquifers. *Water Resour. Res.* **25**, 655–667.

Turner, I. L. & Acworth, R. I. (2004) Field measurements of beachface salinity structure using cross-borehole resistivity imaging. *J. Coastal Res.* **20**(3), 753–760.

Voss, C. I. & Provost, A.M. (2003) A model for saturated-unsaturated, variable-density ground-water flow with solute or energy transport. *US Geol. Survey Water Resour. Invest. Rep*. 02-4231.